Paul E. Hennon[1], **David V. D'Amore**, USDA Forest Service, Pacific Northwest Research Station, 11305 Glacier Highway, Juneau, Alaska 99801,

Dustin T. Witter and **Melinda B. Lamb**, USDA Forest Service, State and Private Forestry, Forest Health Protection, 11305 Glacier Highway, Juneau, Alaska 99801

Influence of Forest Canopy and Snow on Microclimate in a Declining Yellow-cedar Forest of Southeast Alaska

Abstract

Site factors predispose yellow-cedar (*Chamaecyparis nootkatensis* D. Don (Spach)) to a widespread climate-induced mortality in Southeast Alaska. We investigated the influence of canopy cover and snow on microclimate at two small watersheds across a range of declining yellow-cedar stands on Baranof and Chichagof Islands in Southeast Alaska. Two measures of canopy cover, derived from hemispherical photography and LiDAR, were correlated (r = 0.74 and 0.80) at the two sites; both had significant relationships (all $R^2 \geq 0.61$) with basal area of live trees on plots. Reduced canopy cover increases soil warming in spring and leads to rapid changes in air temperature. There is also a positive feedback where the loss of tree overstory due to yellow-cedar mortality contributes to open, exposed site conditions. Variable patterns of snow depth in late winter and spring at one of the sites, documented with daily remote photography, were associated with elevation and cover. Dead trees predominate where lethal shallow soil temperatures occurred but not where snow buffers these temperatures because of existing snow pack. Canopy cover estimates, landscape analysis, and snow modeling could provide the components for a regional risk model to identify areas in Southeast Alaska that are suitable and unsuitable for future conservation and management of yellow-cedar.

Introduction

Yellow-cedar (*Chamaecyparis nootkatensis* D. Don (Spach.)*) has been dying for about 100 years from a widespread mortality in Southeast Alaska known as yellow-cedar decline (Figure 1). Yellow-cedar is a highly valued cultural and economic tree in the region (Hennon and Harris 1997). Wood and bark from yellow-cedar have historical and contemporary cultural value to Native people in British Columbia and Alaska (Stewart, 1984) and its wood is consistently the most commercially valuable of any tree grown in Alaska. Yellow-cedar decline has resulted in about 70% cedar mortality (D'Amore and Hennon 2006) at >2500 mapped locations covering 200,000 ha throughout Southeast Alaska (Snyder and Lundquist 2007). Decline also extends approximately 150 km south on more than 47,000 ha into British Columbia (Hennon et al. 2005, Westfall and Ebata 2009). The lack of understanding of the cause of tree death and the role of site factors has hampered efforts to predict the extent of future mortality and develop conservation and management strategies for this valuable tree species.

Early research examined the possible role of pathogens and other biotic agents and concluded that none was the primary cause of tree death (Hennon et al. 1990b, Hennon and Shaw 1997). We also associated tree mortality with wet, poorly drained sites, but the influence of soil saturation was unknown. Soil drainage patterns affect forest structure and productivity, leading to conditions ranging from bog to dense forest (Neiland 1971), although canopy has not been measured explicitly in the region. Previous research found that air and soil temperatures were significantly associated with the presence of dead cedars which were typically in more open canopy forests (D'Amore and Hennon 2006). Also, we found that yellow-cedar is vulnerable to freezing injury in spring due to its loss of cold hardiness (Hawkins 1993, Hawkins et al. 2001, Schaberg et al. 2005), particularly to fine roots which are killed at <-5 °C (Schaberg et al. 2008).

Interactions of latitude, elevation, and aspect are all associated with yellow-cedar decline (Hennon et al. 2008). At the broadest scale, the distribution of decline aligns with the lowest snow zone in a regional snow map (Hennon et al. 2008). Concen-

[1] Author to whom correspondence should be addressed. Email: phennon@fs.fed.us

* Recently, the taxomomic status of yellow-cedar in the genus *Chamaecyparis* Spach has been questioned due to its affinity with a newly discovered tree species in northern Vietnam (Little et al. 2004).

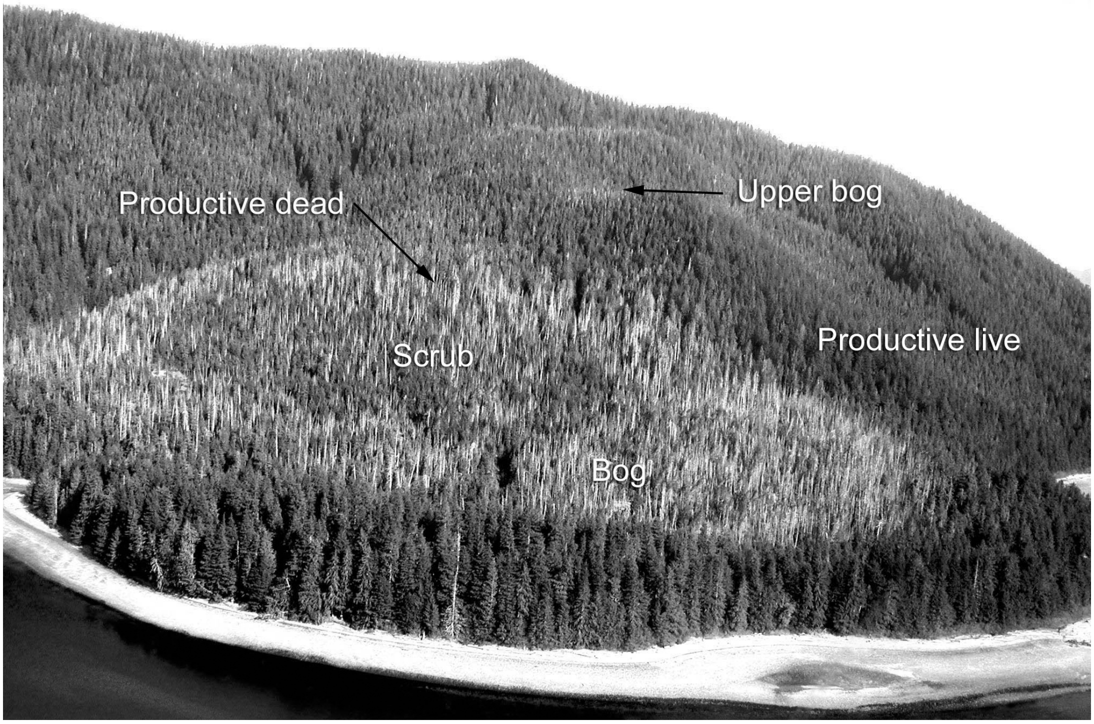

Figure 1. The Poison Cove study site on Chichagof Island, Southeast Alaska, noting zones of forest condition and the appearance of yellow-cedar decline.

trated mortality is limited to lower elevations, but extends to higher elevations on warmer aspects and with decreasing latitude in Alaska and British Columbia (Hennon et al. 2005). These patterns implicate the controlling role of snow in yellow-cedar decline on poorly drained sites. Since 1900, Southeast Alaska has experienced warmer late winter and spring monthly mean temperature, less snow (since 1950 when snow data collection began), but a continuation of periodic freeze-thaw events (Beier et al. 2008).

At the local scale, decline is found on poorly drained soils but yellow-cedar appears healthy where it grows nearby with other conifers on soils with better drainage. Thus, wet soils are considered a risk factor for yellow-cedar decline, but how wet soils interact with canopy structure and microclimate to influence tree health is not understood.

The cumulative knowledge of yellow-cedar decline suggests that many interacting site factors contribute to exposure freezing injury and possible tree death (Figure 2). Previous studies have evaluated some of the steps in this scenario but

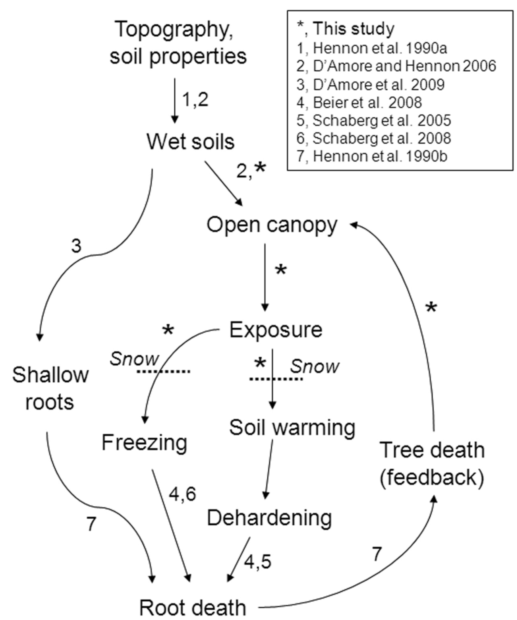

Figure 2. Cascading factors as an explanation for the cause of yellow-cedar decline. The protective role of snow is given. Previous research and the current study used to evaluate each step are noted.

several gaps remain. Canopy cover varies along the forest productivity gradient; however, it has not been quantified using any methods such as canopy photographs or LiDAR in dying forests or elsewhere in the region. The purpose of this paper is to: 1) establish a quantitative relationship of canopy and basal area; 2) describe the relationship among soil moisture, canopy cover, and snow depth; and 3) evaluate how these factors affect air and soil temperature, which appear to lead to injury to yellow-cedar in early spring.

Methods

Site Description and Vegetation Plots

Study plots were established in two small watersheds, Goose Cove (69 plots) and Poison Cove (63 plots). Each watershed was approximately 0.7 km^2 in size. The Goose Cove site, located on Baranof Island (57°30′N, 135°32′W), has a northern aspect and is limited by a ridge at 130 m elevation to the south and west and flanked on the eastern side by poorly drained soils. These watersheds are in roadless areas with no history of timber management. The Poison Cove site (Figure 1), located on Chichagof Island (57°31′N, 135°35′W), has a southerly aspect with a large bowl containing areas of poor drainage at low elevation and another small area of poor drainage at 250 m elevation, which we refer to as "upper bog." A high concentration of dead trees typical of yellow-cedar decline occurs at both watersheds, and each has surrounding forests that appear largely healthy.

Plots were established on systematic grids with 100 m between plots. Live and dead trees $\geq$ 25 cm diameter at breast height (DBH) were measured in 1/30 ha (10.3 m radius) plots; smaller live and dead trees ($\geq$15 cm DBH) were measured in a central, nested plot (1/90 ha, 6.0 m radius). Coordinates for each plot center were initially collected using a GPS device, the PLGR+96 P(Y) coded signal. Positions were averaged for at least 200 measurements and the signal precision was recorded. GPS measurements with poor precision were rejected and replaced with a ground estimated location in the GIS. Plot grids were laid out using a tape, compass, clinometer, and slope correction to facilitate the adjustment of plot positions in GIS. Benchmark locations identifiable in the LiDAR DEM (digital elevation model) were measured again using the Trimble Pro-XR, differentially corrected, and used to further register the plot grid to the LiDAR data. All plot elevation data were obtained from LiDAR measurements. Field tests in similar closed canopy forests achieved accuracies of 2.5 m to 6 m for the PLGR_96 and 2 m to 5 m for the corrected Trimble Pro XR (USDA Forest Service 2000).

Color infrared images at a 1:8000 scale were used to classify vegetation at both study areas (D'Amore and Hennon 2006). Zones of forests were classified visually by the appearance of dead tree concentrations and the apparent degree of canopy closure, resulting in zones mapped as bog (nearly treeless), scrub (open canopy forest), productive dead (previously closed-canopy forest but high concentration of large dead trees), and productive live (closed-canopy forest composed primarily of live trees). Higher ($\geq$150 m) and lower (<150 m) elevations for these zones were distinguished at Poison Cove because of our observation that cedar decline is generally limited to the lower elevations in these areas. The watershed at Goose Cove was all located at low elevation (<150 m) and was thus mapped as the four zones mentioned above.

LiDAR

LiDAR is capable of producing spatially-explicit data for forest canopy structure and is well suited for determining canopy cover (Andersen et al. 2003). The LiDAR data point clouds for both the Goose Cove and Poison Cove watersheds were generated using the 3070 OPTECH ALTM LIDAR system on 13 May 2004. Sub-meter data postings of 0.4 m were achieved with vertical and horizontal accuracy of 15 cm and 60 cm, respectively. Up to four returns, 1st, 2nd, 3rd and last, were collected from each LIDAR pulse. A "bare earth" classification was generated using Terrascan Software. This spatial accuracy and posting density easily supports the sub-meter terrain modeling and forestry applications (Reutebuch et al. 2003). One-meter ground digital elevation models (DEMs) were generated from the bare earth classification using inverse distance weighted (IDW) interpolation in ArcGIS 9.0 (Environmental Systems Research Institute, Inc., Redlands, CA). All-return point data for each plot were combined into a single point cloud. Z values from the underlying ground DEMs were extracted and subtracted from the Z value of each point in the point cloud. The resulting values represented the canopy height structure. All values greater than 2 m were then classified as tree canopy based on our observation that the shrub layer reached to this height in these watersheds. Percent canopy cover was calculated as the points intercepted above the 2 m height threshold relative to the sum of all LiDAR hits. We used all LiDAR returns rather than only first returns to capture small canopy openings at the fine spatial scale of individual plots.

Hemispherical Photographs

Hemispherical photographs directed toward the zenith were taken at each plot on cloudy days in July 2004 with a Nikon FC-E8 fisheye lens on Nikon Coolpix digital cameras mounted on a 1.5 m tripod. The images were oriented on an east-west axis by compass bearing. Images were analyzed with HemiView (Delta-T Devices Ltd., Cambridge, UK) software using manual thresholding (Nobis and Hunzaker 2005) at 32 plots at Poison Cove and 35 plots at Goose Cove. HemiView has been used to document light transmission and solar radiation (Battaglia 2003); however for this analysis, HemiView was used in a more general way to evaluate both of these factors and also influences on snow and temperature. We use the general term canopy cover for estimates produced by HemiView, but recognize that some authors refer to single point view estimates as canopy closure (Jennings et al. 1999).

The images captured a view 180 degrees from the horizontal plane of the lens. Larger viewing angles tend to produce larger values for canopy cover (Bonner 1967). Each environmental variable of interest (e.g., snowfall, solar radiation, heat loss) may require a unique viewing angle. We decreased the viewing angle to 55 degrees, to account for mean tree height of canopy level trees on the perimeter of our 10.3 m radius plots. This angle also includes the maximum percent of incident radiation (Canham et al. 1999) and is related to densitometer measurements and the maximum mean weighted canopy openness (Englund et al. 2000). This provided an exposure measurement that estimated the canopy cover at a minimum tree height of 26 m at the edge of the plot using the gap equation of Leblanc and Fournier (2005).

Snow Occurrence and Depth

Snow depth was measured from photographs taken daily from February until final snow melt at five and eight strategic vegetation plots intended to represent different elevations and canopy conditions at Poison Cove in early spring of 2004 and 2005, respectively. A digital camera was mounted on tree boles in a protective plastic case fitted with a clear window. The camera was connected to a power supply and an intervalometer circuit board that took daily photographs of upright stakes delimited in 10 cm increments from the ground surface. Depth of snow was estimated from the daily photographs of the stakes to the nearest 5 cm.

Temperature

Soil temperatures (15 cm depth) and surface air temperatures (10 cm above ground) were recorded at four-hour intervals with automated devices (Hobo Temperature Pro, Onset Computer Corp., Bourne, MA) at 30 plots at the Poison Cove site from September 2003 to June 2005. Other devices were used in 13 selected plots to represent the classified forest zones to record soil temperature at 7.5 and 15 cm depths at four-hour intervals and air temperature hourly at 2 m above ground. Cables were housed in rigid plastic tubing to protect them from rodents, but some devices failed to produce data due to water infiltration. Some data were lost from temperature devices and snow camera installations due to destruction by bears. Analysis of some temperature data focused on the two winter and spring measurements because these periods represent the timing of yellow-cedar vulnerability driven by dehardening and freezing injury (Schaberg et al. 2005, 2008). Using a minimum threshold of 0 °C, cumulative 'degree days' were calculated from four-hour interval soil data for March through May as an indication of warming in early spring.

$$DD = \sum(T°/6)$$

Where DD = degree days (°C)

T° = temperature (°C) is >0 °C, every four hours (6 intervals / day)

Statistical Analysis

The numbers of plots with tree, canopy, and microclimate data are summarized in Table 1. Data from vegetation plots were used to calculate estimates of basal area for both live and dead standing trees to relate with values of canopy cover derived from LiDAR and hemispherical photographs at the same plots. Pearson Correla-

TABLE 1. Number of plots where tree, canopy, and microclimate data were recorded at the two study sites in Alaska.

	Poison Cove	Goose Cove
Live and dead trees	63	69
Hemispherical photographs	32	35
LiDAR	32	35
Air temp. (2 m) [a]	12,11	-
Air temp. (ground, 10 cm) [a]	25,22	-
Soil temp. (15 cm depth) [a]	25,22	-
Soil temp. (7.5 cm depth) [a]	11,10	-
Snow depth [a]	5,7	-

[a] Two values are given where different number of plots with microclimate data were recorded in the first and second years, respectively.

tion Coefficient (Corr Procedure, SAS Institute 2004) was used to test the correlation between canopy estimates from LiDAR and hemispherical photographs. Simple regression (GLM Procedure, SAS Institute 2004) was used to test the relationship between each of these estimates and live basal area from plots. Multiple regressions (GLM Procedure, SAS Institute 2004) tested the inclusion of dead tree basal area ($P \leq 0.1$) with live tree basal area in models with the two estimates of canopy cover. Multiple regression was also used to test the significance of canopy cover (from hemispherical photographs) and elevation in predicting ground air and soil (15 cm depth) degree days from the months of March through May. Explanatory variables were included in each model where $P \leq 0.1$. Differences in canopy cover estimates derived from hemispherical photographs and LiDAR in the classified forest zones were tested with analysis of variance and multiple comparisons (GLM Procedure and Bonferroni's method, SAS Institute 2004). All differences were judged to be significant at $P \leq 0.05$ and analyses were conducted separately for Poison Cove and Goose Cove.

Results

Canopy

Canopy cover estimates from hemispherical photographs and LiDAR were significantly correlated at Poison Cove and Goose Cove (both P<0.0001, r = 0.74, r = 0.80). LiDAR produced greater canopy cover estimates (10 to 89 %) than hemispherical photographs (0 to 85 %), particularly in plots with low basal area (Figure 3). More mid- and lower-canopy vegetation is sensed by LiDAR, especially at the periphery of the plot, than hemispherical photographs because of the different detection methods of each technology. Increasing the viewing angle from 55 to the full

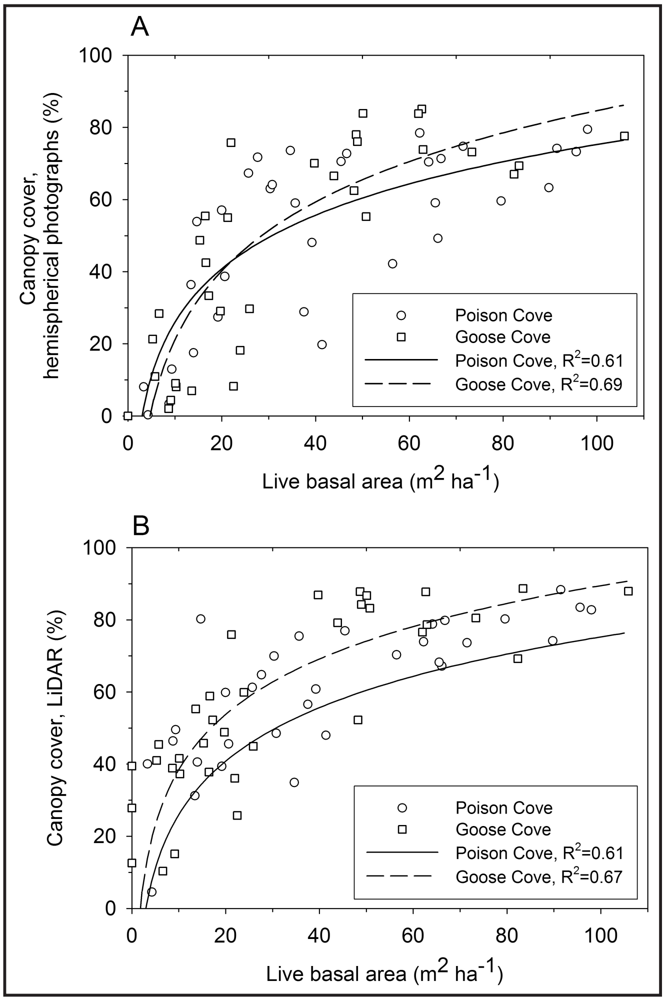

Figure 3. Relationship of live tree basal area and canopy cover estimates from A) hemispherical photographs, and B) LiDAR at two watersheds in Southeast Alaska.

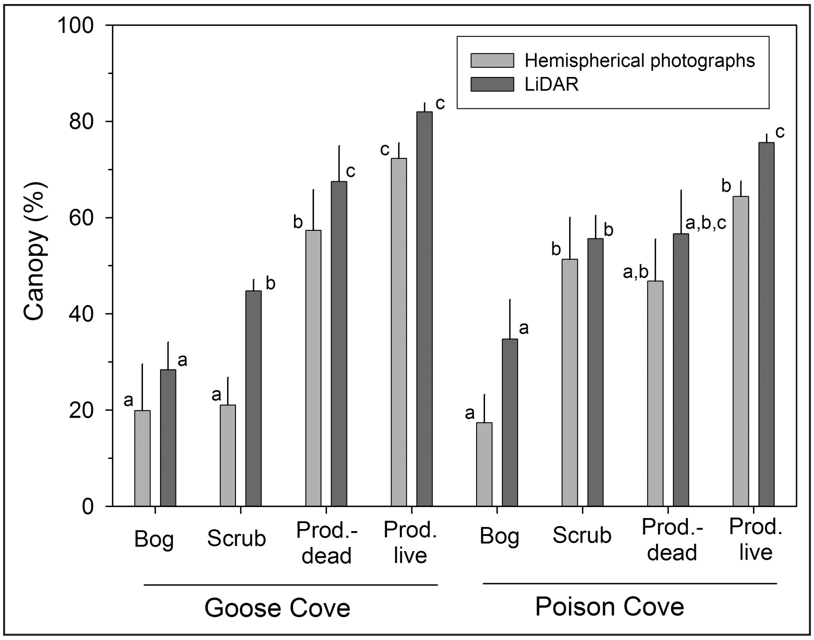

Figure 4. Mean canopy cover measured by hemispherical photographs and LiDAR for the four classified forest zones at Goose Cove and Poison Cove. Bars are standard errors. Different letters denote significant differences between forest zones for each canopy estimation technique.

180 degrees in hemispherical photographs created the opposite effect: it produced greater cover estimates relative to LiDAR due to the capture of increased vegetation and topography. The use of multiple return LiDAR data appeared to better record small canopy openings and provided a better fit with hemispherical photos than if cover estimates were limited to first returns only. Forest zones (i.e., classified from aerial photographs) had significantly different levels of canopy cover as estimated by hemispherical photographs and LiDAR (all $P < 0.006$), although individual zones were not always different from one another (Figure 4). There was an increase in canopy along the bog-to-productive-forest gradient; however, this trend was disrupted by the variability in canopy cover in the scrub plots (Figure 4).

Canopy cover estimates from hemispherical photographs and LiDAR had significant relationships with live tree basal area at both sites (all $R^2 \geq 0.61$, Figure 3) based on a log-normal transformation of basal area. The distribution of residuals and increased R^2 suggest a curvilinear relationship: increasing basal area produced smaller changes in plots that approached full canopy cover.

Both branches and boles of dead standing trees were clearly observed on many of the hemispherical photographs and were considered components of cover. Multiple regression demonstrated that dead tree basal area contributed to canopy cover, along with live tree basal area. Dead basal area was a significant factor in cover models derived from LiDAR (P = 0.007) and hemispherical photographs (P = 0.09) at Poison Cove, but not for either method (P = 0.57, 0.18, respectively) at Goose Cove (Table 2). These results were consistent with the generally greater concentrations of dead yellow-cedar trees at Poison Cove than Goose Cove. The total basal areas (i.e., live + dead) of 78 and 72 $m^2\,ha^{-1}$ in the productive dead zones of Poison and Goose Cove, respectively, were similar to the adjacent live forests of 72 $m^2\,ha^{-1}$ at both sites. The high concentrations of dead trees in the productive dead zones (49 and 39 $m^2\,ha^{-1}$ at Poison and Goose Cove, respectively) represent considerable cover reduction due to the loss of branches and foliage. Most of the surviving trees, and thus canopy cover, were surviving western hemlock and mountain hemlock in these zones.

TABLE 2. Partial results from multiple regressions of canopy cover derived from hemispherical photographs and LiDAR, and explanatory variables (live tree basal area and dead tree basal area) at the two study sites in Alaska.

	Model			Live Tree Basal Area	Dead Tree Basal Area
Canopy Cover	n[a]	R^2	*P* value	*P* value	*P* value
Hemisph. photos					
Poison Cove	32	0.50	0.0001	0.0001	0.09
Goose Cove	32	0.66	0.0001	0.0001	0.18
LiDAR					
Poison Cove	32	0.67	0.0001	0.0001	0.007
Goose Cove	35	0.64	0.0001	0.0001	0.57

[a] Number of plots used in model

Snow

Daily photographs of snow depth in late winter and spring of 2004 and 2005 revealed the influence of elevation and forest canopy on snow deposition and melt (Figure 5). Although the higher elevation plots are less than 300 m above sea level, snow there was considerably deeper and persisted more than a month longer than the lower elevation plots. A snow event in late March, 2004 covered the ground with about 10 cm of snow at low elevation plots, but the snow only persisted for several days. Snow that occurred in late March 2005 in and near the upper bog plot was not evident at lower elevation plots. No snow was detected in a low elevation plot with full canopy while nearby low elevation bog and scrub plots had intermittent snow in late winter, 2005, illustrating the role of canopy in intercepting snow. Generally, snow persisted longer into spring 2004 than 2005, but temperature data (below) revealed that periods in late winter before our snow cameras were installed (i.e., before mid February) had more persistent snow in the first winter than the second.

Temperature and Freeze-thaw

Periodic cold periods in both winters monitored at Poison Cove were evident, with air temperatures < -5 °C and occasionally <-10 °C (Figure 6). Sub freezing daily minimum air temperatures occurred in April during both springs. Mean soil temperatures at 15 cm depth were always above freezing, even during the brief, but cold, (< -10 °C) events (Figure 6).

Shallow soil temperatures (7.5 cm deep) were much more responsive to air temperatures than deeper soils and reached lower minima, but only when there was no snow cover (Figure 7). Shallow soil temperatures from both live and dead plots followed air temperature in early winter 2004, when there was no snow present. The cold event in late January 2004 produced very cold shallow soil temperatures in the dead plots without snow, but temperatures remained near zero in the live higher elevation plots with snow. The presence of snow delayed soil warming by approximately two months in the higher elevation live plots in 2004. Most severe cold events occurred early in the second winter and early spring when snow appeared to buffer shallow soil temperatures. Sub-freezing soil temperatures were not reached during the last brief cold event in March of the second spring (2005), apparently due to warmer soil temperatures that preceded the event in the lower elevation dead plots and the presence of snow in the healthy upper bog plots. Cumulative 15-cm deep soil temperatures were significantly related to elevation and/or canopy cover at different times from March through May in 2004 and 2005 (Table 3). Elevation was a significant explanatory factor in each of the three months in 2004 but only March in 2005. Canopy cover only became significant by May 2004 and by April and May of 2005. The greater influence of canopy cover in 2005 than in 2004 was probably due to the warmer spring in 2005 (Figure 6). When significant, soil degree days were negatively related to both higher elevation and greater canopy cover.

Results of multiple regression of ground air temperature by elevation and canopy cover (not shown in Table 3) had similar results but higher R^2 values (0.58 to 0.73 for 2004, 0.29 to 0.43 for 2005). For ground air temperature (10 cm above ground), elevation was a significant explanatory factor in all six of these models, but canopy cover was significant for March 2005 only. One cold

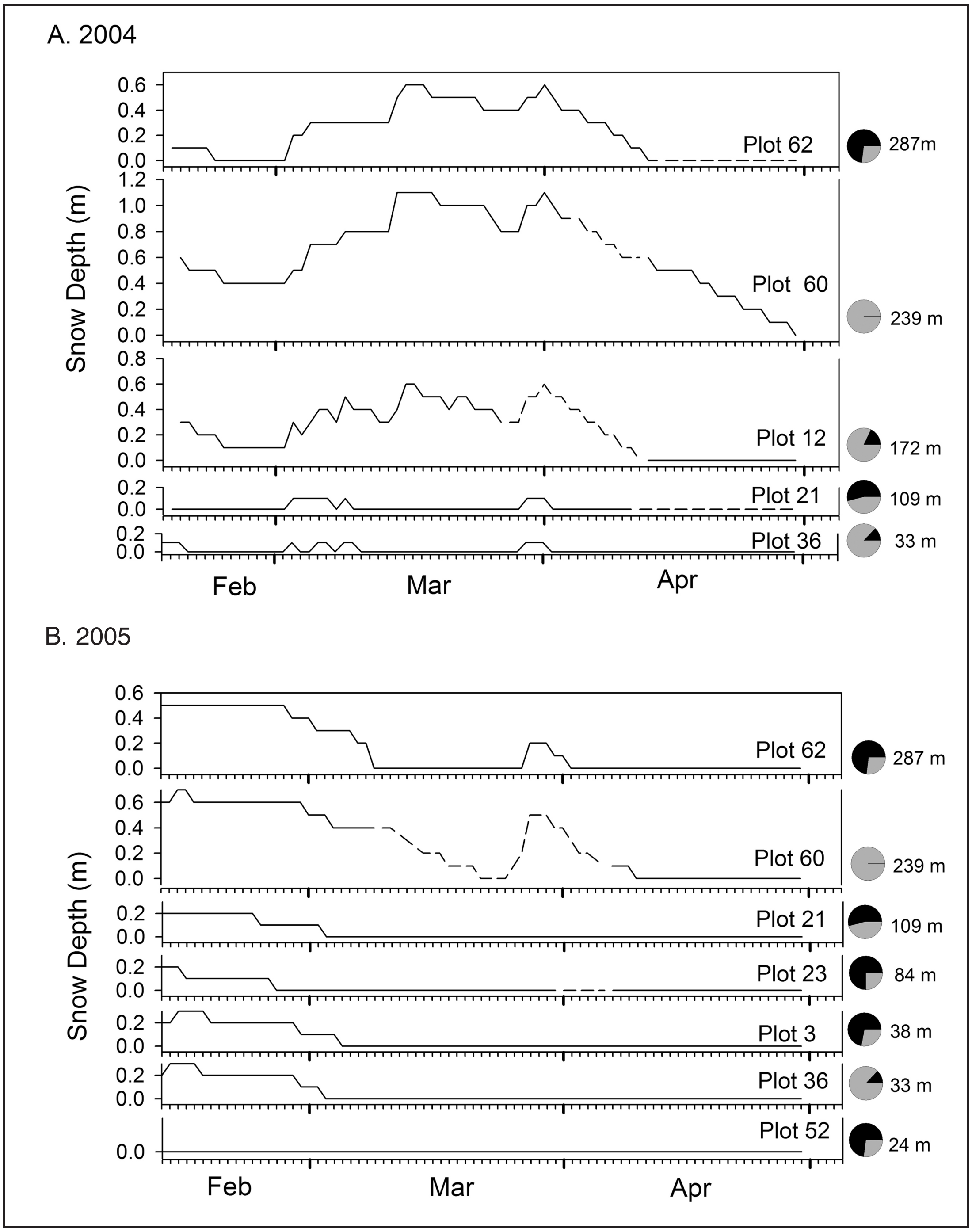

Figure 5. Snow depth on selected plots at the Poison Cove site during spring of 2004 (A) and 2005 (B). Solid lines are from daily digital photographs; dashed lines represent interpreted values (from soil temperatures, patterns of snow depth on similar plots, or direct observation) during periods of battery malfunction or equipment damage by bears. Circular symbols to the right indicate percent open (light grey) and closed canopy (black) from hemispherical photographs, followed by elevation of the plot in meters.

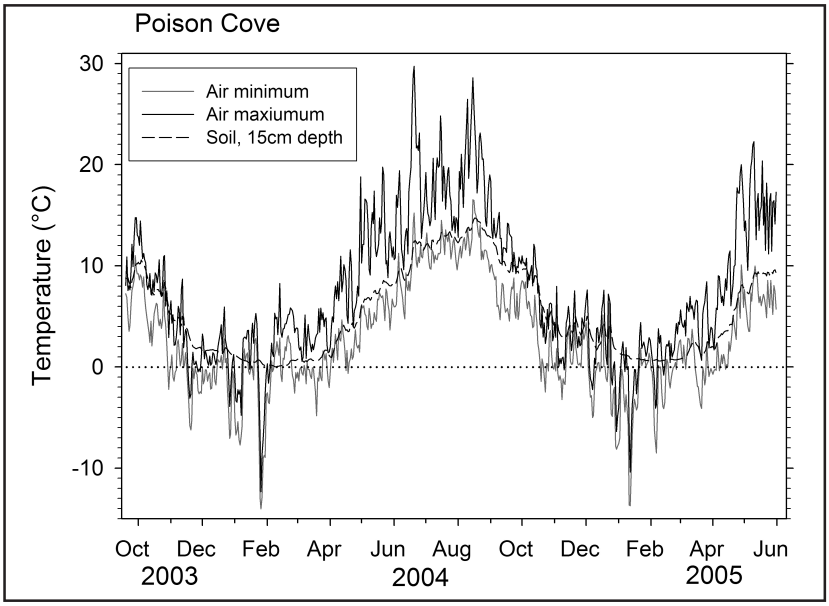

Figure 6. Mean minimum and maximum daily air temperature (recording hourly) and mean soil temperature (15 cm depth, recording every four hours) from 22 temperature logging devices at Poison Cove, Chichagof Island, Alaska.

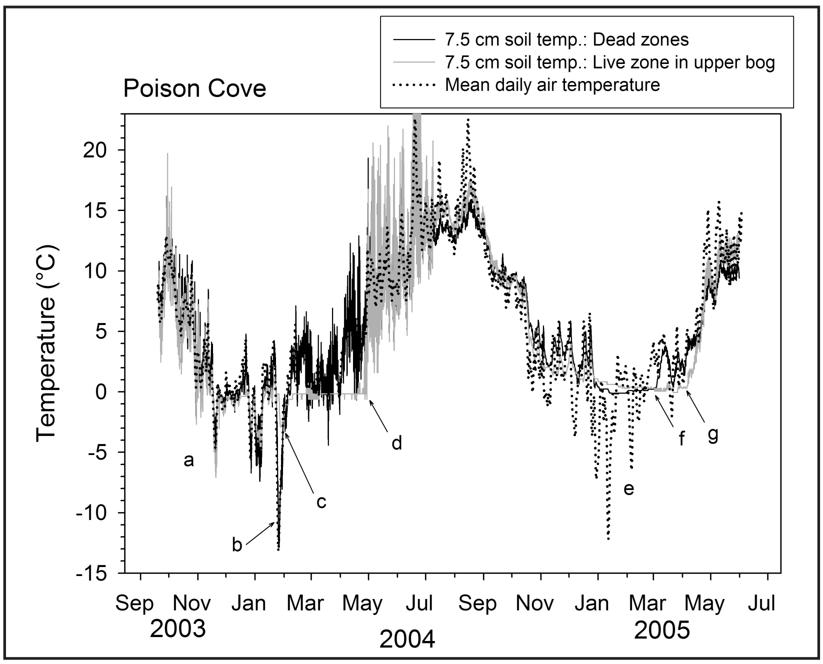

Figure 7. Shallow soil temperature (7.5 cm depth) at plots representing dead zones (low elevation bog, scrub, and productive dead, n=6) and upper (higher elevation) bog and scrub which are healthy (n=5). Daily temperature (at 2 m height, mean from all zones, n=7). Notes: a) snow absent early in 2003-2004 winter, b) example of damaging soil temperature in dead zone, c) damaging temperature buffered by snow in live zone with snow, d) delayed soil warming due to snow in live zone, e) snow present in all zones in winter of 2004-2005 buffered soil from cold air temperature, f) earlier snow melt in dead zone, and g) later snow melt in the live zone.

TABLE 3. Partial results from multiple regressions of cumulative soil degree days (15 cm depth) > 0˚C from March through May and explanatory variables elevation and canopy cover on plots at Poison Cove, Chichagof Island, Alaska.

Soil Degree Days		Model n^b	Model R^2	Model *P* value	Elevation *P* value	Canopy Cover *P* value
2004	March	25	0.15	0.16	0.09	0.44
	April	25	0.40	0.003	0.001	0.33
	May	25	0.36	0.006	0.005	0.07
2005	March	22	0.15	0.20	0.09	0.62
	April	20	0.23	0.09	0.51	0.05
	May	20	0.24	0.09	0.93	0.03

[a] Canopy cover is percent canopy from hemispherical photographs analyzing the 55 degree viewing angle from the center of each plot.

[b] Number of plots used in model

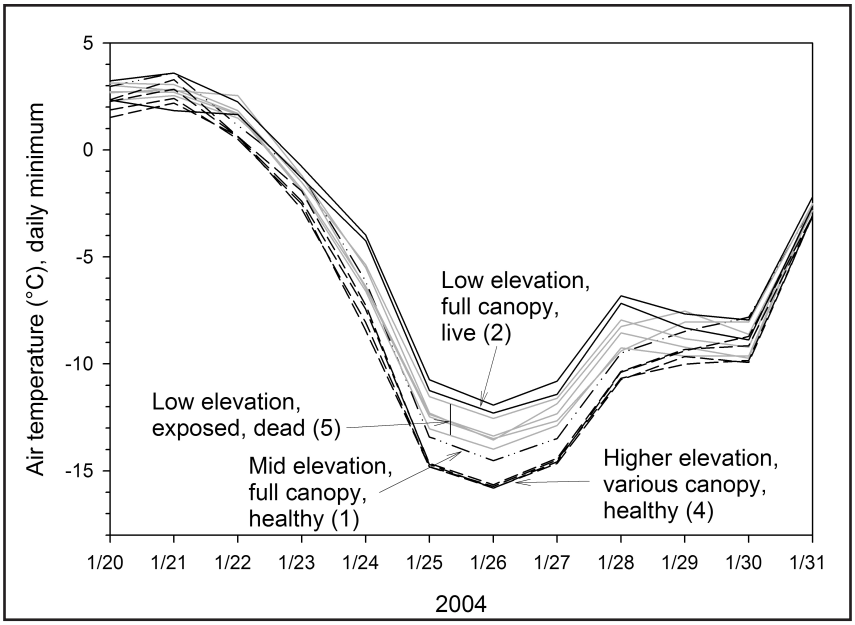

Figure 8. Air temperature (2 m above ground) during a cold period from plots with different elevations and degree of forest canopy. Values in parentheses are numbers of plots.

period in January 2004 was used to examine the influence of canopy on minimum temperatures (Figure 8). Air temperature differed little among plots at several elevations and amount of canopy cover before and after the cold event. During the coldest days, however, low elevation-closed canopy plots were approximately four degrees warmer than the high elevation plots. The low elevation, exposed plots were intermediate.

Elevation and canopy cover also influenced shallow (7.5 cm) cumulative soil degree days (Figure 9). Lower elevation, open canopy (bog) plots experienced earlier and greater warming. Closed canopy, low elevation forest plots had a slower rate of warming. Upper elevation bog and forest plots showed a delay in the onset of warming due to snow. Once initiated, after snowmelt, soil warming was rapid, particularly in the open bog plot.

Discussion

Our study demonstrated the complex interaction of topography, canopy, and snow in influencing air and soil temperature. These findings are consistent

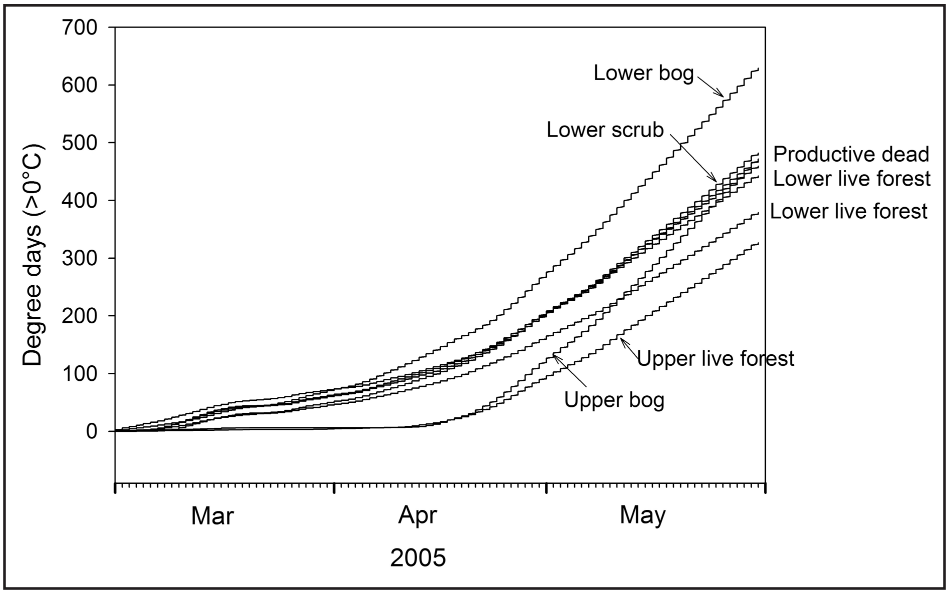

Figure 9. Cumulative soil degree days (>0 °C) for shallow (7.5cm deep) soil temperatures from March through May 2005 for selected plots at Poison Cove, Chichagof Island, Alaska. See text for description of the forest zones.

with the pattern of yellow-cedar decline on the landscape and our interpretation of the contributing roles of these site factors in the cause of yellow-cedar decline. Open canopy conditions, measured by hemispherical photography and LiDAR in the bog and scrub zones, existed before the onset of yellow-cedar decline. Mortality of trees in adjacent areas then converted these areas to a more open canopy condition. Dead trees contribute far less canopy cover than live trees due to loss of foliage and branches. Thus, the recently-killed trees serve as a source of feedback that promotes further decline where warming through exposure may trigger dehardening of yellow-cedar tissues (Schaberg et al. 2005). Exposure creates greater extremes in microclimate: ground air temperatures reach higher daily maxima and slightly lower minima in exposed conditions. Soil warming in spring, as expressed by degree days, is greater in exposed areas because of increased solar radiation. The presence of snow prevents the cascading factors thought to lead to tree death by 1) delaying soil warming which may trigger dehardening in yellow-cedar roots, and/or 2) buffering soil temperatures so that the lethal threshold value of < -5 °C is not reached. Where snow persists past the last cold event in spring, yellow-cedar is not thought to suffer root freezing injury.

The measurement of forest canopy and elevation provides one of the primary means to predict risk of tree injury in yellow-cedar forests. Hemispherical photographs and LiDAR estimated canopy cover with similar results, confirming the ability of each to detect fine-scale changes in canopy cover (i.e., plots). LiDAR produced somewhat higher canopy cover estimates than hemispherical photos, however. This inconsistency could be attributed to the choice of a 2 m height threshold for estimating cover as well as the finite size of the laser used in LiDAR. The 2 m threshold was chosen because it is roughly the height of the taller shrubs. LiDAR would have intersected some low cover above this height on the periphery of our plots not captured by the conical view of hemispherical photos from a single point. Our use of the 55 degree viewing angle eliminated the direct influence of slope on the hemispherical photographs (i.e., ground upslope counting as cover), but correcting for terrain in this analysis would provide more refined estimates of cover. The size of the laser path (potentially up to 1 m) may also capture more cover than the small pixels available in hemispherical photography analysis. Manipulating the 2 m threshold in the LiDAR analysis or the 55 degree conical viewing angle in the hemispherical photography analysis can greatly alter the resulting canopy cover values estimated by each technique. These issues have been somewhat resolved in recent work (Zhao and Popescu 2009), but for the present study the relationship provides a good, though not exact agreement for mapping canopy cover. Future research on estimating canopy cover in the forests of Southeast Alaska should investigate these factors to refine the results presented here.

The small deviations in the estimates derived from hemispherical photographs compared to LiDAR imply that this method is a cost-effective approach as a surrogate to LiDAR coverage on small plots, especially in the productive forest type where the methods produced similar values. LiDAR produces superior vertical structure for forest canopies and has the advantage of estimating slope, aspect, and canopy cover across large areas (Popescu et al. 2002, Andersen et al. 2005).

Both cover estimates confirm the strong influence of soil drainage (i.e., gradient of bog to well developed forest) in limiting overstory productivity and reducing canopy cover (Zach 1950, Lawrence 1958, Neiland 1971, Klinger 1996). Saturated soils reduce aerobic mineralization of nitrogen and phosphorous, leading to reductions in tree vigor and biomass accumulation. These drainage gradients along hillslopes lead to a broad range of vegetation response in the plots, influencing canopy cover from completely open to approximately 90 % closed. The dense overlapping canopy layers in well developed forests contributed to the non-linear relationship between the basal area of live trees and cover estimates, where increasing basal area created minimal gains in canopy cover. Small scale disturbance, often through single tree mortality, creates the canopy gaps that temporarily increase light transmission and allow understory development (Alaback 1984, Gray et al. 2002).

Yellow-cedar has been competitive in poorly-drained soils where it is particularly abundant fringing open peatlands (Neiland 1971). The potential adaptation to acquire nitrate-nitrogen through shallow fine rooting has been proposed as the means for cedars to maintain a competitive advantage in poorly-drained soils (D'Amore et al. 2009). This adaptation also leaves yellow-cedar susceptible to freezing injury, especially in exposed landscape positions such as open canopy areas. The oldest zones of decline are typically found immediately adjacent to open areas where some trees that died up to 100 years ago are still standing (Hennon et al. 1990a, D'Amore and Hennon 2006). Mortality progresses upward along the drainage gradient into better drained soils and denser canopies where tree death has been more recent than in the central wetter zones (D'Amore and Hennon 2006). The progression of decline from small to large diameter trees has a corresponding increase in the loss of canopy cover. Basal area values of dead trees from the "productive dead" zones in declining yellow-cedar forests suggest that a closed canopy existed before intensive tree mortality, but these large dead trees still provide some cover in areas with concentrations of standing snags. Thus, yellow-cedar decline spreads from areas with hydrologically-controlled low canopy cover to adjacent trees thereby increasing exposure. The concentration of trees dying from the decline syndrome produces a new feedback mechanism for creating open canopy conditions (e.g., the periphery of the mortality zone in Figure 1).

The extent of canopy cover, responding to the long-term drainage gradient and tree mortality, exerts influence over ground air and soil temperatures, particularly by attenuating increases in temperatures. Soils supporting less canopy cover warm more quickly in late winter than heavily shaded forests as a result of increased solar radiation. Thus, the greater heat capacity of wet soils (Jury et al. 1991) has less direct influence on soil warming than does the open canopy condition. The presence of snow, however, maintains isothermal soil temperatures despite varying canopy cover. Exposed soils at all elevations in Southeast Alaskan forests can develop frozen layers to greater than 30 cm deep, but these frost depths are shallower in areas with deep forest litter or snow accumulation (Patric 1967). Soil under accumulated snow may be initially frozen, but soil temperatures just under the snow are held near 0 °C, eventually allowing the soil to thaw from below due to upward heat flux from deeper soil layers toward the surface. Soil warming, as expressed by cumulative degree days, does not show any marked increase until the snow melts, exposing the surface to solar radiation. Yellow-cedar is predisposed to deharden earlier than western hemlock in the spring (Schaberg et al. 2005), presumably to provide a competitive advantage by rapid growth and acquisition of nitrates once snow melts (D'Amore et al. 2009). Therefore, a persistent spring snow pack may protect yellow-cedar by preventing early soil warming and subsequent dehardening.

Canopy cover also influences snow pack through interception and insulation (D'Eon 2004). Snow depth was previously found to be negatively related to canopy cover, and measures of tree basal area and tree volume in Southeast Alaska (Hanley and Rose 1987, Kirchhoff and Schoen 1977). We found the same relationship of less snow with greater canopy cover on our plots; however, with increasing elevation, snow pack occurs even under dense canopies, as in forested plots near the upper bog plots at Poison Cove. These results imply that elevation has a greater influence than canopy closure on snow cover and thus soil temperature. Sites at higher elevations than we sampled (i.e., >287 m) would be expected to have more consistent and deeper snow cover, later final melt in spring, and a corresponding delay in soil warming.

Recent research by Schaberg et al. (2008) reported a cold tolerance threshold for yellow-cedar roots of -5°C in late winter. If soil temperatures fall below this temperature, yellow-cedar roots can be damaged through freezing injury. We rarely recorded these lethal soil temperatures around deeper roots (>15 cm), but <-5°C was common in the shallow root zone at 7.5 cm depth. Snow cover prevents these lethal temperatures at any rooting depth even during periods of very cold air temperature. In Southeast Alaska, yellow-cedar roots will be protected where snow persists through April, or beyond the last hard freeze of the spring. This protective function of snow for yellow-cedar roots likely explains the pattern of yellow-cedar decline at three spatial scales: 1) decline aligns with low snow levels on a regional snow map (Beier et al. 2008), 2) decline has elevational limits but appears somewhat higher on warmer aspects at the mid scale (Hennon et al. 2008), and 3) decline occurs in open canopy stands at our two watersheds, except in the upper bog area at Poison Cove (this study). Healthy yellow-cedar forests on wet soils, similar to the upper bog community at Poison Cove, occur in the vicinity of our study watersheds, but they are always found at higher elevations than the declining cedar forests. In a dendrochronological study of yellow-cedar, Beier et al. (2008) provided evidence of more stable radial growth during the Little Ice Age, which ended in the late 1800s, a time that coincided with the onset of yellow-cedar decline (Hennon et al. 1990a). The ages of live and dead yellow-cedar trees in declining forests indicate that most regenerated during this snowy period (Viens 2001) of the Little Ice Age (Hennon and Shaw 1994), conceivably becoming abundant in the low elevation areas where they are now dying.

Our finding of exposure as an important risk factor in yellow-cedar decline is now integrated into our proposed conservation strategy (Hennon et al. 2008) for this valuable tree species. The proposed conservation strategy considers how soil drainage, canopy cover, and snow interact to create vulnerable and favorable locations on the landscape for yellow-cedar. Thus, canopy cover combined with landscape attributes such as slope, soil type, and elevation provide the components for a risk model that designates suitable and unsuitable areas for yellow-cedar conservation and management. Salvage harvest of dead yellow-cedar produces valuable wood products (Hennon et al. 2007) and may remove some harvesting pressure from healthy cedar forests. Our conservation strategy recommends harvesting some of the dead yellow-cedar in areas of existing decline while favoring other tree species that are better suited to conditions in these declining forests. Our strategy also identifies areas that would be suitable to promote yellow-cedar through active management, such as planting and thinning. These favorable areas are 1) in well drained soils where roots grow more deeply and canopy shading buffers temperature extremes, and 2) where spring snow is adequate to protect roots until the last cold period has passed in spring. Management aimed at promoting a long-lived tree species must account for continued climate warming and altered patterns of spring snow, however. Thus, we are incorporating predictions of climate change and projected snow patterns into landscape models to identify areas suitable for long term management of this valuable forest tree.

Acknowledgements

We wish to thank Tom Heutte for assistance in developing the snow cameras. We appreciate Jason Fellman and Jacob Berkowitz who tirelessly assisted with field work, and Tim Max for statistical guidance throughout this study. Troy Heithecker, Hans Andersen, Steve Reutebuch, and anonymous reviewers made helpful suggestions on drafts of this manuscript.

Literature Cited

Alaback, P. B. 1984. A comparison of old-growth forest structure in the western hemlock-Sitka spruce forests of southeast Alaska. *In* Fish and Wildlife Relationships in Old-growth Forests: Proceedings of a Symposium, 12-15 April 1982, Juneau, Alaska, American Institute of Fishery Research Biologists. Pp. 219-226.

Andersen, H. -E., R. J. McGaughey, and S. E. Reutebuch. 2005. Estimating forest canopy fuel parameters using LIDAR data. Remote Sensing of Environment 94:441-440.

Andersen, H. -E., R. J. McGaughey, W. Carson, S. Reutebuch, B. Mercer, and J. Allan. 2003. A comparison of forest canopy models derived from LIDAR and INSAR data in a Pacific Northwest conifer forest. International Archives of Photogrammetry and Remote Sensing 34(3):211-217.

Battaglia, M. A., R. J. Mitchell, P. P. Mou, and S. D. Pecot. 2003. Light transmittance estimates in a longleaf pine woodland. Forest Science 49:752-762.

Beier, C. M., S. E. Sink, P. E. Hennon, D. V. D'Amore, and G. P. Juday. 2008. Twentieth-century warming and the dendroclimatology of declining yellow-cedar forests in southeastern Alaska. Canadian Journal of Forest Research 38:1319-1334.

Bonner, G.M. 1967. Estimation of ground canopy density from ground measurements. Journal of Forestry 65:544-547.

Canham, C. D., D. Coates, P. Bartemucci, and S. Quaglia. 1999. Measurement and modeling of spatially explicit variation in light transmission through interior cedar-hemlock forests of British Columbia. Canadian Journal of Forest Research 29:1775-1783.

D'Amore, D. V., and P. E. Hennon. 2006. Evaluation of soil saturation, soil chemistry, and early spring soil and air temperatures as risk factors in yellow-cedar decline. Global Change Biology 12:524-545.

D'Amore, D. V., P. E. Hennon, P. G. Schaberg, and G. Hawley. 2009. Adaptation to exploit nitrate in surface soils predisposes yellow-cedar to climate change-induced decline while enhancing the survival of western redcedar: a new hypothesis. Forest Ecology and Management 258:2261-2268.

D'Eon, R. G. 2004. Snow depth as a function of canopy cover and other site attributes in a forested ungulate winter range in southeast British Columbia. BC Journal of Ecosystems and Management 3:136-144.

Englund, S. R., J. J. O'Brien, and D. B. Clark. 2000. Evaluation of digital and film hemispherical photography and spherical densitometry for measuring forest light environments. Canadian Journal of Forest Research 30:1999-2005.

Gray, A. N., T. A. Spies, and M. J. Easter. 2002. Microclimate and soil moisture responses to gap formation in coastal Douglas-fir forests. Canadian Journal of Forest Research 32:332-343.

Hanley, T. A., and C. L. Rose. 1987. Influence of overstory on snow depth and density in hemlock-spruce stands: Implications for management of deer habitat in southeastern Alaska. Research Note PNW-RN-459. USDA Forest Service, Pacific Northwest Research Station, Portland, OR.

Hawkins, B. J. 1993. Photoperiod and night frost influence the frost hardiness of *Chamaecyparis nootkatensis* clones. Canadian Journal of Forest Research 23:1408-1414.

Hawkins, B. J., J. H. Russell, and J. Arnott. 2001. Cold hardiness of yellow-cedar (*Chamaecyparis nootkatensis* (D. Don) Spach). *In* F. J. Bigras and S. J. Colombo (editors), Conifer Cold Hardiness, Kluwer, Netherlands. Pp. 531-554.

Hennon, P. E., A. S. Harris. 1997. Annotated bibliography of *Chamaecyparis nootkatensis*. Gen. Tech. Rep. PNW-GTR-413. U.S. Dep. Agric., Pacific Northwest Research Station, Portland, OR. 112 p.

Hennon, P. E., D. D'Amore, D. Wittwer, and J. Caouette. 2008. Yellow-cedar decline: conserving a climate-sensitive tree species as Alaska warms. *In* R. Deal (editor). Integrated Restoration of Forested Ecosystems to Achieve Multiresource Benefits: Proceedings of the 2007 National Silviculture Workshop. Gen. Tech. Rep. PNW-GTR-733. U.S. Department of Agriculture, Forest Service, Pacific Northwest Research Station, Portland, OR. Pp. 233-245.

Hennon, P. E., D. V. D'Amore, S. Zeglen, and M. Grainger. 2005. Yellow-cedar decline in the North Coast Forest District of British Columbia. Research Note PNW-RN-549. U.S. Department of Agriculture, Forest Service, Pacific Northwest Research Station, Portland, OR.

Hennon, P. E., E. M. Hansen, and C. G. Shaw III. 1990a. Dynamics of decline and mortality of *Chamaecyparis nootkatensis* in southeast Alaska. Canadian Journal of Botany 68:651-662.

Hennon, P. E., C. G. Shaw III, and E. M. Hansen. 1990b. Symptoms and fungal associations of declining *Chamaecyparis nootkatensis* in southeast Alaska. Plant Disease 74:267-273.

Hennon, P. E., and C. G. Shaw III. 1994. Did climatic warming trigger the onset and development of yellow-cedar decline in southeast Alaska? European Journal of Forest Pathology 24:399-418.

Hennon, P. E., and C. G. Shaw III. 1997. The enigma of yellow-cedar decline: what is killing these defensive, long-lived trees in Alaska? Journal of Forestry 95:4-10.

Hennon, P. E., B. Woodward, and P. K. Lebow. 2007. Deterioration of wood from live and dead Alaska yellow-cedar in contact with soil. Forest Products Journal 57(6):23-30.

Jennings, S. B., N. D. Brown, and D. Sheil. 1999. Assessing forest canopies and understory illumination: canopy closure, canopy cover, and other measures. Forestry 72:59-73.

Jury, W., W. R. Gardner, and W. H. Gardner. 1991. Soil Physics. 5th Edition. John Wiley and Sons, New York. 352 p.

Kirchhoff, M. D., and J. W. Schoen. 1987. Forest cover and snow: implications for deer habitat in southeast Alaska. Journal of Wildlife Management 51:28-33.

Klinger, L. F. 1996. Coupling of soils and vegetation in peatland succession. Arctic and Alpine Research 28:380-387.

Lawrence, D. B. 1958. Glaciers and vegetation in southeastern Alaska. American Scientist 46:89-122.

Leblanc, S. G., and R. A. Fournier. 2005 Towards a better understanding of in-situ canopy measurements used in the derivation and validation of remote sensing leaf area index products. *In* 31st International Symosium on Remote Sensing of the Environment, June 20-24, St. Petersburg, FL. Available from http://www.isprs.org/publications/related/ISRSE/html/papers/909.pdf. [Accessed 3 January 2009].

Little, D. P., A. E. Schwarzbach, R. P. Adams, and C. F. Hsieh. 2004. The circumscription and phylogenetic relationship of *Callitropsis* and the newly described genus *Xanthocyparis* (Cupressaceae). American Journal of Botany 91:1872-1881.

Neiland, B. J. 1971. The forest-bog complex of southeastern Alaska. Vegetatio 22:1-64.

Nobis, M., and U. Hunziker. 2005. Automatic thresholding for hemispherical canopy-photographs based on edge detection. Agricultural and Forest Meteorology 128:243-250.

Patric, J. H. 1967. Frost depth in forest soils near Juneau, Alaska. Research Note PNW-RN-60. USDA Forest Service, Pacific Northwest Research Station, Portland, OR.

Popescu, S. C., R. H. Wynne, and R. F. Nelson. 2002. Estimating plot-level tree heights with lidar: local filtering with a canopy-height based variable window size. Computers and Electronics in Agriculture 37(1-3):71-95.

Reutebuch, S. E., R. J. McGaughey, H. E. Andersen, and W. W. Carson. 2003. Accuracy of a high-resolution LIDAR terrain model under a conifer forest canopy. Canadian Journal of Remote Sensing 29:527–535.

SAS Institute Inc. 2004. General Linear Models Procedure. SAS OnlineDoc 9.1.3. Cary, NC: SAS Institute Inc.

Schaberg, P. G., P. E. Hennon, D. V. D'Amore, G. J. Hawley, and C. J. Borer. 2005. Seasonal differences in freezing tolerance of yellow-cedar and western hemlock trees at a site affected by yellow-cedar decline. Canadian Journal of Forest Research 35:2065-2070.

Schaberg, P. G., P. E. Hennon, D. V. D'Amore, and G. J. Hawley. 2008. Influence of simulated snow cover on the cold tolerance and freezing injury of yellow-cedar seedlings. Global Change Biology 14:1282-1293.

Stewart, H. 1984. Cedar: Tree of Life to the Northwest Coast Indians. University of Washington Press, Seattle, WA.

Snyder, C., and J. Lundquist. 2007. Forest health conditions in Alaska—2006. Protection Report R10-PR-11. U.S. Department of Agriculture Forest Service, Alaska Region, Juneau, AK.

USDA Forest Service. 2000. Comparison of GPS receivers under a forest canopy with selective availability off. [online]. Available from http://www.fs.fed.us/database/gps/mtdcrept/documents/comsaoff.doc. [Accessed 30 July 2008].

Viens, R. J. 2001. Late Holocene climate change and calving glacier fluctuations along the southwestern margin of the Stikine Icefield, Alaska. Ph.D. Dissertation, University of Washington, Seattle.

Westfall, J., and T. Ebata. 2009. 2008 summary of forest health conditions in British Columbia. British Columbia Ministry of Forests and Range. Pest Management Report No. 15. 76 p.

Zach, L. W. 1950. A northern climax, forest or muskeg? Ecology 31:304-306.

Zhao, K., and S. Popescu. 2009. Lidar-based mapping of leaf area index and its use for validating GLOBCARBON satellite LAI product in temperate forest of the southern USA. Remote Sensing of Environment 113: 1628-1645.

Received 7 April 2009
Accepted for publication 12 October 2009